DP-MS-89-27

MICROSTRUCTURE AND YIELD STRENGTH EFFECTS ON HYDROGEN AND TRITIUM INDUCED CRACKING IN HERF STAINLESS STEEL (U)

by

M. J. Morgan and M. H. Tosten
Westinghouse Savannah River Company
Savannah River Site
Aiken, SC 29808

Author's Signature:

A paper for presentation at a meeting on the
Hydrogen Effects on Material Behavior
Jackson Lake Lodge
Moran, WY
September 12-16, 1989

and for publication in the proceedings of the meeting

Derivative Classifier J. P. Howell - Manager
Signature and Title

DP-MS-89-27

MICROSTRUCTURE AND YIELD STRENGTH EFFECTS ON HYDROGEN AND TRITIUM INDUCED CRACKING IN HERF STAINLESS STEEL (U)

by

M. J. Morgan and M. H. Tosten
Westinghouse Savannah River Company
Savannah River Site
Aiken, SC 29808

A paper for presentation at a meeting on the
Hydrogen Effects on Material Behavior
Jackson Lake Lodge
Moran, WY
September 12-16, 1989

and for publication in the proceedings of the meeting

MICROSTRUCTURE AND YIELD STRENGTH EFFECTS ON HYDROGEN AND TRITIUM INDUCED CRACKING IN HERF STAINLESS STEEL

Michael J. Morgan and Michael H. Tosten

Westinghouse Savannah River Company
Savannah River Site
Aiken, SC 29808

Abstract

Rising-load J-integral measurements and falling-load threshold stress intensity measurements were used to characterize hydrogen and tritium induced cracking in high-energy-rate-forged (HERF) 21-6-9 stainless steel. Samples having yield strengths in the range 517-930 MPa were thermally charged with either hydrogen or tritium and tested at room temperature in either air or high-pressure hydrogen gas. In general, the hydrogen isotopes reduced the fracture toughness by affecting the fracture process. Static recrystallization in the HERF microstructures affected the material's fracture toughness and its relative susceptibility to hydrogen and tritium induced fracture. In hydrogen-exposed samples, the reduction in fracture toughness was primarily dependent on the susceptibility of the microstructure to intergranular fracture and only secondarily affected by yield strength in the range of 660 to 930 MPa. Transmission-electron microscopy observations revealed that the microstructures least susceptible to hydrogen-induced intergranular cracking contained patches of fully recrystallized grains. These grains are surrounded by highly deformed regions containing a high number density of dislocations. The microstructure can best be characterized as "duplex", with soft recrystallized grains embedded in a hard, deformed matrix. The microstructures most susceptible to hydrogen-induced intergranular fracture showed no well-developed recrystallized grains. The patches of recrystallized grains seemed to act as crack barriers to hydrogen-induced intergranular fracture. In tritium-exposed-and-aged samples, the amount of static recrystallization also affected the fracture toughness properties but to a lesser degree. In these samples, fracture occurred by transgranular, quasi-cleavage through the heavily-deformed grains in the unrecrystallized microstructures and by cracking along the grain boundaries in the recrystallized microstructures. The different dislocation substructures and their effects on the trapping of tritium and its radioactive decay product, helium, are the apparent causes of the two different fracture modes.

This article was prepared in connection with work done under Contract No. DE-AC09-76SR00001 with the U. S. Department of Energy.

Introduction

High-energy-rate-forged (HERF) austenitic stainless steels are used as the materials of construction for vessels designed for the containment of hydrogen and its isotopes. Embrittlement of these materials by hydrogen has been a source of concern for some time. The nature and the degree of embrittlement by hydrogen varies considerably and, among other factors, is a complicated function of material composition and processing variations (1-5). Although the exact physical process that is responsible for the embrittlement of steels by hydrogen is still debated, the attainment of a local enrichment of hydrogen within microstructural interfaces along with the application of a critical stress level are almost certainly required.

Helium, the radioactive decay product of tritium, will also embrittle stainless steels. Precipitation of microscopic helium bubbles tends to increase the material's strength as well as weaken interfaces like grain and twin boundaries. Since fracture toughness tends to decrease with increasing yield strength, at least part of the helium-embrittlement problem may be due to strength effects. The relationship between a material's initial yield strength and toughness and the incremental strength increase and the corresponding toughness decrease imparted by helium is not known.

The purpose of this study was to measure the combined effects of strength, hydrogen isotopes, and helium on the mechanical and fracture toughness properties of HERF stainless steel.

Experimental Procedure

Mechanical property and fracture toughness data were measured using samples machined from four sets of 21-6-9 stainless steel forgings in the form of forward-extruded cylinders which were about 10 cm long and a 3.8 cm diameter. The forgings had been high-energy-rate-forged to produce nominal yield strengths of 660, 760, 870, and 930 MPA. A few samples from each forging were subsequently annealed to produce a nominal yield strength of 517 MPa. The heat compositions and the forging and annealing treatments are given in Table I. Tensile samples were cut longitudinally from the forgings and C-shaped fracture toughness samples were cut from the transverse orientation. The tensile samples had a 25.4 mm gage length and a 4.8 mm diameter. The C-specimens had an inside radius of 9.65 mm, an outside radius of 18.8 mm, and a thickness of 4.57 mm. The C-shaped specimens were fatigue pre-cracked per ASTM 399 guidelines prior to testing (6).

TABLE I Heat Compositions and Forging Treatments

	Heat Compositions (w/o)									
Heat[a]	Cr	Ni	Mn	P	Si	C	S	N	O(ppm)	Al
1	19.2	7.22	9.23	.014	.41	.032	.003	.28	19	.002
2	19.4	6.40	8.50	.021	.33	.040	<.001	.28	22	<.001
3	20.1	6.50	9.10	.019	.59	.037	<.001	.29	10	.001

[a] Heat 1 was used for forgings of nominal yield strengths of 660 and 760 MPa.
Heat 2 was used for forgings of nominal yield strengths of 760 and 870 MPa.
Heat 3 was used for forgings of nominal yield strengths of 930 MPa.

Forging Conditions: Extrusion die and stub punch; heat parts to 1255 K +/- 10 K; hold for 10 to 15 minutes; forge 1 blow at 2 MPa +/- .17 MPa; water quench; heat to 1116 K +/- 10 K; forge 1 blow at 5.5 MPa +/- .17 MPa; water quench.

Annealing Conditions (Nominal Yield Strength of 517 MPa): 1144 K for 5-6 min.

One set of samples was exposed to hydrogen gas at 623 K and 69 MPa for 6 weeks. This treatment saturated the samples with approximately 9500 appm hydrogen based on available diffusivity and solubility data (5). Another set of samples was exposed to tritium gas at 423 K and 31 MPa for 9 months, and aged for 12 more months at 298 K for helium build-in from tritium decay. In the C-specimens the calculated average tritium and helium concentrations were 1600 appm and 150 appm respectively. In the tensile specimens the average tritium and helium concentrations were calculated to be 2470 appm and 390 appm helium respectively.

The samples were pulled at room temperature in air or in 10000 psi hydrogen gas using a screw-driven testing machine and a crosshead speed of 0.0085 mm/s. Two fracture toughness measurement techniques were used; falling-load, threshold-stress intensity (Kth) and rising-load, J-integral measurements. K_{th} was measured by holding the samples in the "fixed-grip" condition and recording the drop in load from crack growth over a 24 to 48 hour period. K_{th} was calculated from the final crack length (measured on heat-tinted fracture surfaces), the final load, and the K-calibration equation for the C-specimen given in ASTM E399-83 (6). Crack growth rates for $K > K_{th}$ were estimated from the theoretical compliance relationship (7). Rising-load J-integral data were obtained by pulling precracked samples to failure, assuming crack initiation at maximum load and using the area under the load-loadline displacement curve to calculate the J-integral toughness. J-integral measurements using the unloading compliance technique (7) could not be performed in the high-pressure hydrogen experiments because of friction effects in the seals. These J-integral values were in general agreement with those obtained from unloading-compliance for control samples.

Transmission electron microscopy (TEM) specimens were sectioned from the C-specimens by cutting thin wedge-shaped slices radially equivalent to the fracture plane. These slices were mechanically ground to a uniform thickness of about 0.38 mm and subsequently punched into 3 mm diameter discs. Thin foils were prepared in a Struers' Tenupol jet-polishing apparatus using a solution of 1 part H_2SO_4: 7 parts methanol at 15V and 253 K. All TEM was performed with a Philips EM400T operating at 120 kV.

Results

The mechanical properties of the hydrogen-exposed, tritium-exposed, and control samples are shown in Fig. 1. Over the range of yield strengths from 517 to 930 MPa, the samples containing 9500 appm hydrogen showed on average 33% lower ductilities and 11% higher yield strengths than the control samples. The tritium-exposed-and-aged samples showed 46% lower ductilities and 9% higher yield strengths than the controls. The ductility decrease and the strength increase observed in the HERF (unannealed) tritium-exposed samples was roughly equivalent to the hydrogen-exposed samples even though the hydrogen isotope concentration was 75% lower. This is due to the presence of helium from the radioactive decay of tritium. Note that the tritium-exposed samples that were annealed prior to the tritium exposure and testing (i.e., 517 MPa yield strength) had the lowest ductilities.

The effects of hydrogen and tritium on the rising-load fracture toughness properties are shown in Fig. 2. All control samples fractured by a microvoid nucleation and growth process. In the control samples the fracture toughness decreased by more than 43% as the yield strength increased from 660 to 930 MPa. In the samples containing 9500 appm hydrogen and pulled in 69 MPa hydrogen gas, the fracture toughness values were reduced, but the level of reduction depended on the response of the microstructure to the hydrogen.

In about half of the samples tested, hydrogen simply assisted the strain-controlled microvoid nucleation and growth fracture process and the rising-load fracture toughness values were about 20% lower than the control samples. On many of these samples, fractography indicated smaller void sizes and spacings than those observed in the control samples. In the remaining samples hydrogen changed the microscopic fracture process to a stress-controlled intergranular fracture process. In these samples the fracture toughness was about 72% lower on average.

Similar effects were observed in the falling load threshold stress intensity measurements. For example, in one 870 MPa sample held in the fixed grip condition in 69 MPa hydrogen gas, hydrogen caused slow crack growth along the grain boundaries with a K_{th} of 67.0 MPa-$m^{1/2}$. In another 870 MPa sample, slow crack growth was not observed after step loading to an applied stress intensity as high as 121 MPa-$m^{1/2}$.

Optical and transmission-electron microscopy observations did not indicate any sensitization variations in the samples; however, other differences in the microstructures of the "good" and "bad" (high and low toughness) materials were observed. Examples of these observations are shown in Figs. 3-5. The most obvious differences are that the "good" material contains regions of fully recrystallized grains. These grains are surrounded by highly deformed regions containing a high number density of dislocations. The resulting microstructure can best be characterized as "duplex", with "soft" recrystallized grains embedded in a "hard" matrix. It is estimated that in the specimens examined, the volume recrystallized is approximately twenty to thirty percent. Recrystallization most likely occurred during or subsequent to the last forging blow. This is evidenced by the low number of dislocations observed within the recrystallized grains and the absence of dislocations in the annealing twin boundaries that are present. It should be noted that small recrystallization nuclei were observed in the "bad" material, however, no well-developed grains were found. These "soft" recrystallized grains in the good material apparently serve as barriers to crack propagation and make it more difficult for hydrogen-induced intergranular fracture to occur.

The effects of tritium and its decay product, helium, on the rising-load fracture toughness properties are also shown in Fig. 2. These samples were pulled in air and contained about 1600 appm tritium and 150 appm helium. Although the hydrogen-isotope content was just 17% of the hydrogen-exposed samples, the fracture toughness values were reduced to about the same level as those measured in the "bad" microstructures cited above. As was observed in the hydrogen-exposed samples, microstructural variations in the forgings led to two different fracture paths in these samples. However, unlike the hydrogen-exposed samples, falling-load experiments indicated that both were stress-controlled fracture modes.

One of these failure modes is shown in Fig. 6(a) and is a quasi-cleavage fracture through a microstructure with elongated grains. The absence of secondary cracking like that observed in the hydrogen-induced fracture in Fig. 3 indicates that this fracture mode is transgranular rather than intergranular or interfacial. Other samples failed by grain-boundary cracking in a microstructure with fine, equiaxed grains. An example is shown in Fig. 6(b). This latter microstructure apparently resulted from static recrystallization during forging. Most samples showed fracture along a combination of these two paths. TEM observations confirmed that recrystallized grains were present in the samples which fractured along the grain boundaries. Also, Fig. 7 shows that, in the tritium-containing samples, helium bubbles are trapped in the cores of dislocations.

Falling-load threshold stress intensity measurements on the tritium-exposed and aged samples showed similar effects and some of the results are shown in Fig. 8. In these figures the applied stress intensity is plotted against the compliance-calculated crack growth rates. As shown by example in Fig. 8(a), only a small effect of yield strength on K_{th} was observed: K_{th} of 92.3 MPa-$m^{1/2}$ in the 660 MPa sample versus 85.7 MPa-m in the 870 MPA sample. Both of these samples showed slow crack growth along ultra-fine grain boundaries. A much larger effect of microstructure on K_{th} was observed. This is shown by the two 870 MPa data shown in Fig. 8(b). One sample failed by 100% quasi-cleavage at a threshold of 63.7 MPa-$m^{1/2}$; the other failed by grain-boundary cracking with a threshold of 85.7 MPa-$m^{1/2}$. Both of these cracking processes occurred in the fixed-grip tests under a falling load and so were stress-controlled.

The crack velocities seemed to speed up and slow down a number of times during these experiments. This was detected by a series of changes in the rate of load drop with time and results in the oscillations seen in the Stage II portions of the crack velocity vs. stress intensity data in Fig. 8. These oscillations could be due to microscopic cracks linking up with the main crack or perhaps reflect the cracking process being controlled by tritium migration. A more sensitive crack growth measuring technique than the technique used here is probably necessary to explore these anomalies.

Discussion

The results presented above illustrate a number of important effects. First, hydrogen isotopes and helium increased the yield strength and reduced the fracture toughness properties of HERF 21-6-9 stainless steel. Helium was more effective than hydrogen in changing these properties. Figs. 1 and 2 indicate that the fracture toughness reductions caused by helium were not simply a consequence of its

effect on strength. The fact that many of the tritium-exposed samples exhibited a transgranular fracture mode that was not observed in the hydrogen-exposed samples supports this observation as well.

Secondly, the amount of static recrystallization that occurs during the high-energy-rate-forging process plays a very important role in the response of the material to hydrogen and tritium. In the samples containing hydrogen, a microstructure consisting of isolated patches of recrystallized grains surrounded by heavily worked grains resulted in relatively high fracture toughness properties. The "soft" recrystallized grains apparently act as barriers to hydrogen-induced intergranular fracture. In contrast, in hydrogen-exposed samples that contained very few recrystallized grains the fracture mode was nearly 100% intergranular.

Finally, in samples containing tritium and helium from tritium decay, the amount of static recrystallization also affected the fracture toughness properties but to a lesser degree. These samples failed by transgranular, cleavage-like cracking in heavily deformed microstructures and intergranular cracking in recrystallized microstructures. The different helium and tritium distributions in these two microstructures is probably the cause of the two different fracture modes. TEM observations indicated that helium from tritium decay was trapped as microscopic bubbles in the cores of dislocations. These bubbles must act as additional traps for tritium. The tritium and helium trapped in and around the cores of dislocations in the heavily-deformed microstructures would then induce quasi-cleavage by lowering cohesion along the slip planes. In the recrystallized grains, the tangles of dislocations are not available as traps for the helium and tritium. In these microstructures, tritium and helium can more easily migrate in these microstructures by diffusion or dislocation transport to the grain boundaries, lower cohesion, and causes intergranular fracture. These tritium and helium distribution effects would also explain the low ductility of the annealed and fully recrystallized (517 MPa yield strength) tensile samples.

Summary

Hydrogen isotope and helium effects on the mechanical and fracture toughness properties of a high-energy-rate-forged stainless steel were investigated. The results indicated that variations in the HERF microstructure because of static recrystallization during the forming process were much more important than yield strength in the cracking behavior of this material. In the case of hydrogen, patches of recrystallized grains seemed to act as crack barriers to hydrogen-induced cracking. In the case of tritium, static recrystallization altered the helium and tritium distributions and thus changed the crack path from transgranular fracture in "cold-worked" microstructures to intergranular fractures in the recrystallized microstructures.

References

1. A. W. Thompson, "The Mechanism of Hydrogen Participation in Ductile Fracture", *Effect of Hydrogen on Behavior of Materials*, eds., A. W. Thompson and I. M. Bernstein (AIME 1977), 467-477.

2. B. C. Odegard, J. A. Brooks, and A. J. West, "The Effect of Hydrogen on the Tensile Behavior of Nitrogen Strengthened Stainless Steel", *ibid*, 116-125.

3. J. A. Brooks and A. J. West, "Hydrogen-Induced Ductility Losses in Austenitic Stainless Steel Welds" Metall. Trans A, 12A (1981), 213-223.

4. C. L. Briant, "Hydrogen-Assisted Cracking of Type 304 Stainless Steel," Metall. Trans A, 10A (1979), 181-189.

5. G. R. Caskey, Jr., "Hydrogen Effects in Stainless Steels," Hydrogen Degradation of Ferrous Alloys, eds. J.P. Hirth, R. W. Oriani, and M. Smialowski, (Park Ridge, NJ: Noyes Publications, 1985), 822-862.

6. "ASTM E399-83: Standard Test Method for Plane-Strain Fracture Toughness of Metallic Materials", Annual Book of ASTM Standards, vol 3.01, 680-715.

7. "ASTM E813-87: Standard Test Method for J_{Ic}, A Measure of Fracture Toughness", Annual Book of ASTM Standards, vol 3.01, 968-990.

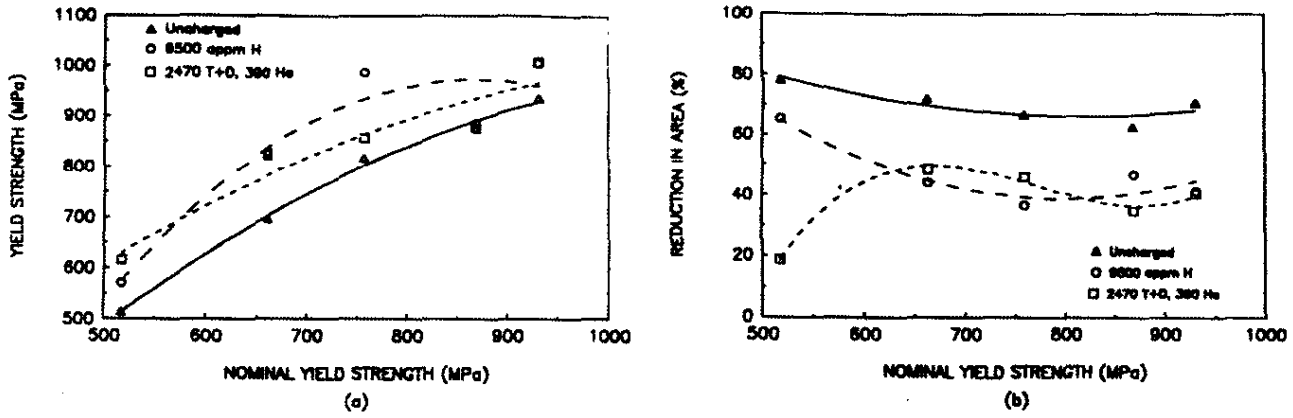

Fig. 1. Hydrogen and Tritium Effects on Mechanical Properties: (a) Yield Strength; (b) Ductility.

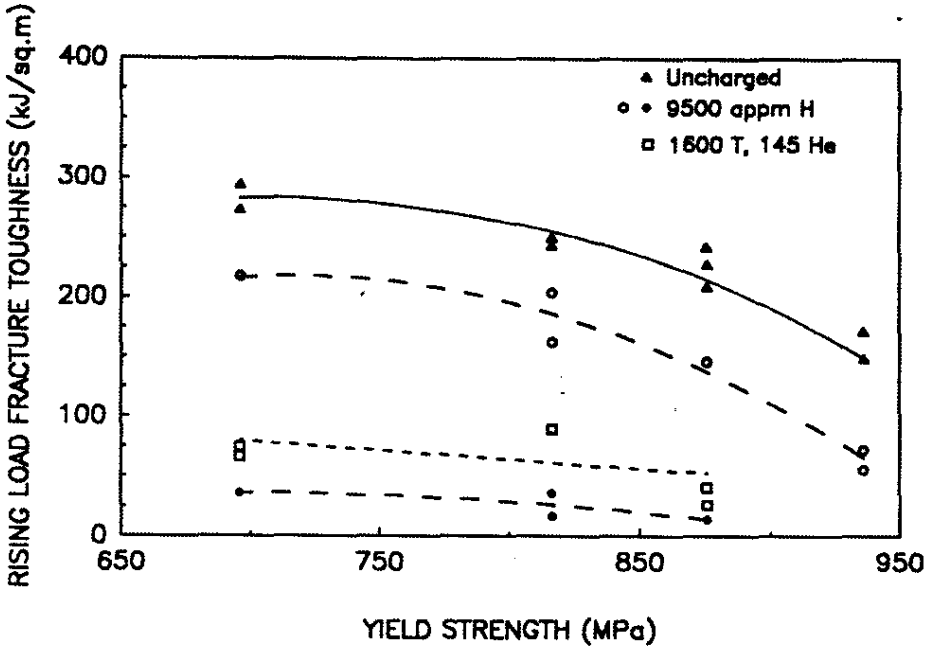

Fig. 2. Hydrogen and Tritium Effects on Rising-Load J-Integral Fracture Toughness.

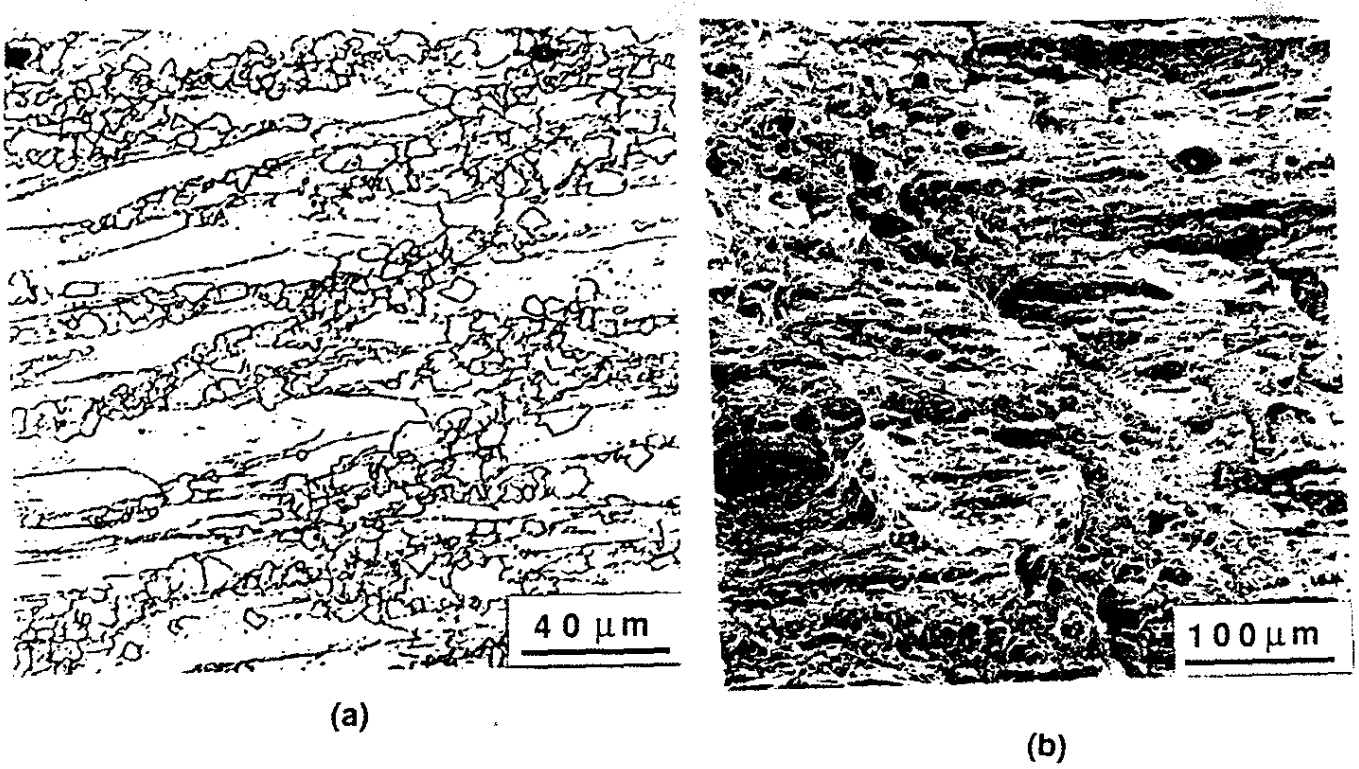

Fig. 3. Hydrogen-Assisted Strain-Controlled Fracture in High-Toughness HERF Microstructure. (a) Partially-Recrystallized Microstructure; (b) Dimpled Rupture.

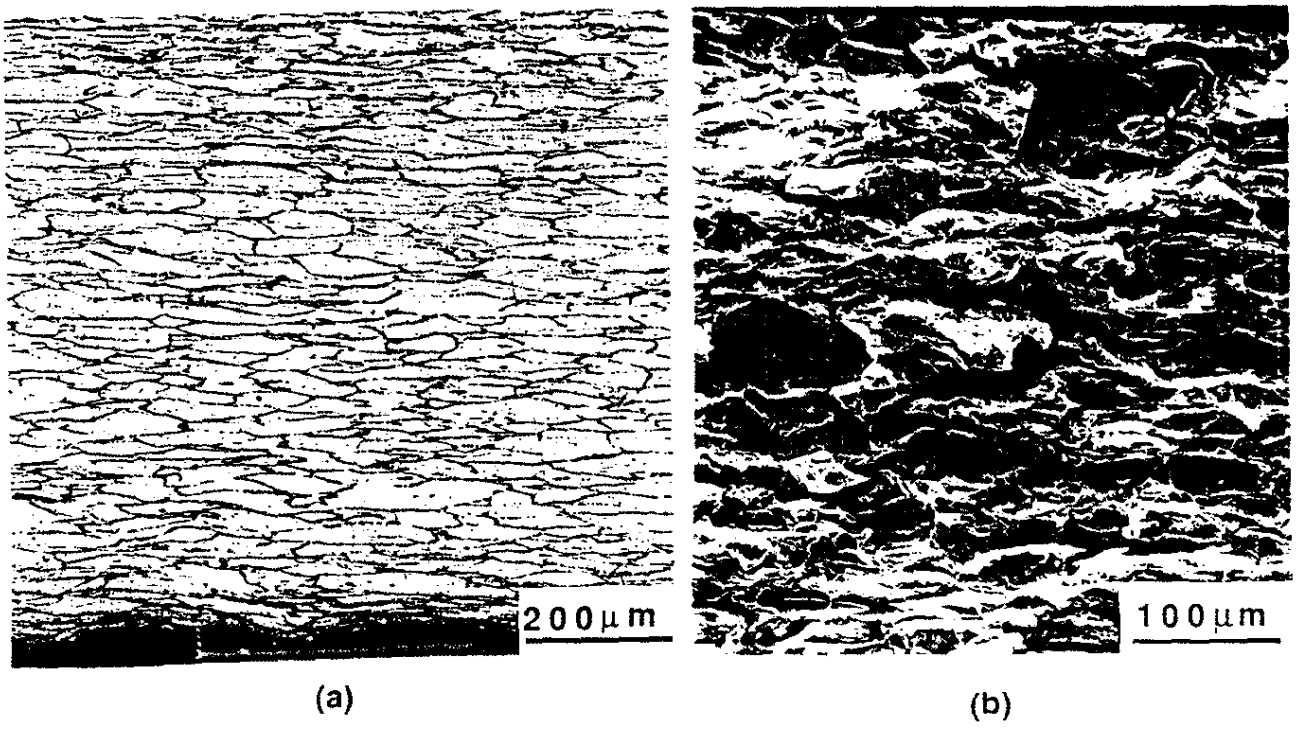

Fig. 4. Hydrogen-Induced Stress-Controlled Intergranular Fracture in Low-Toughness HERF Microstructure. (a) Unrecrystallized Microstructure; (b) Intergranular Fracture.

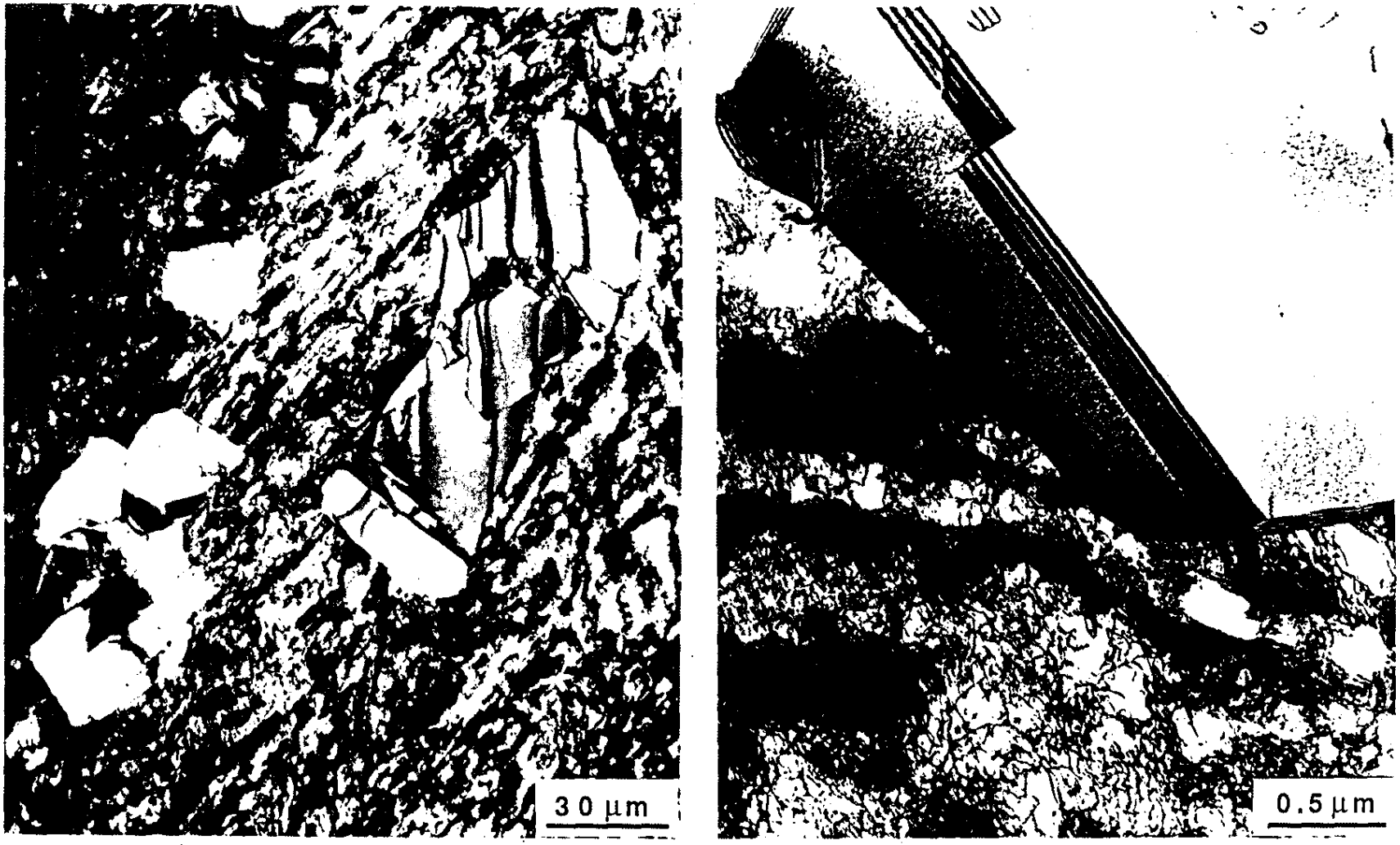

Fig. 5. Patches of Recrystallized Grains Surrounded by Deformed Grains in High-Toughness Microstructure.

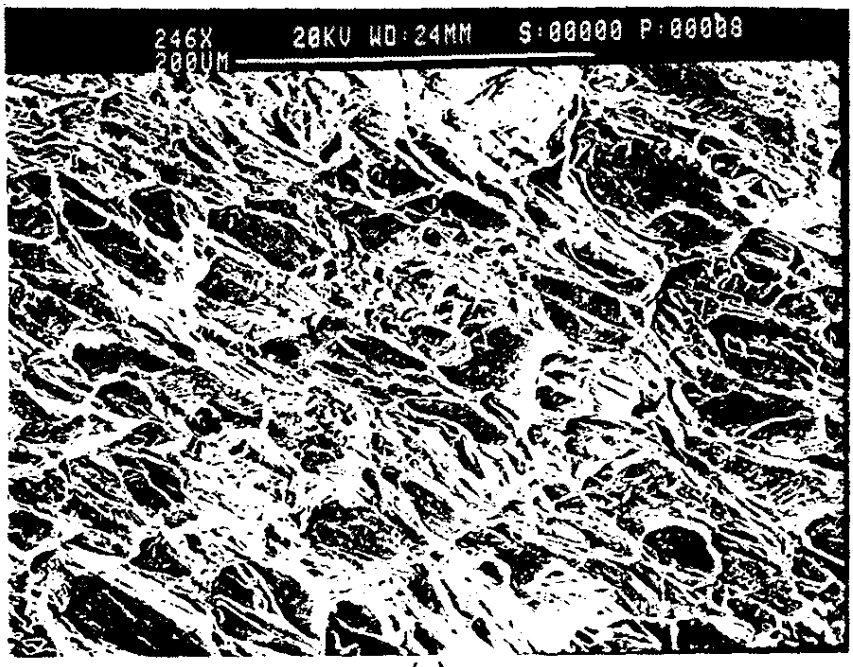

(a)

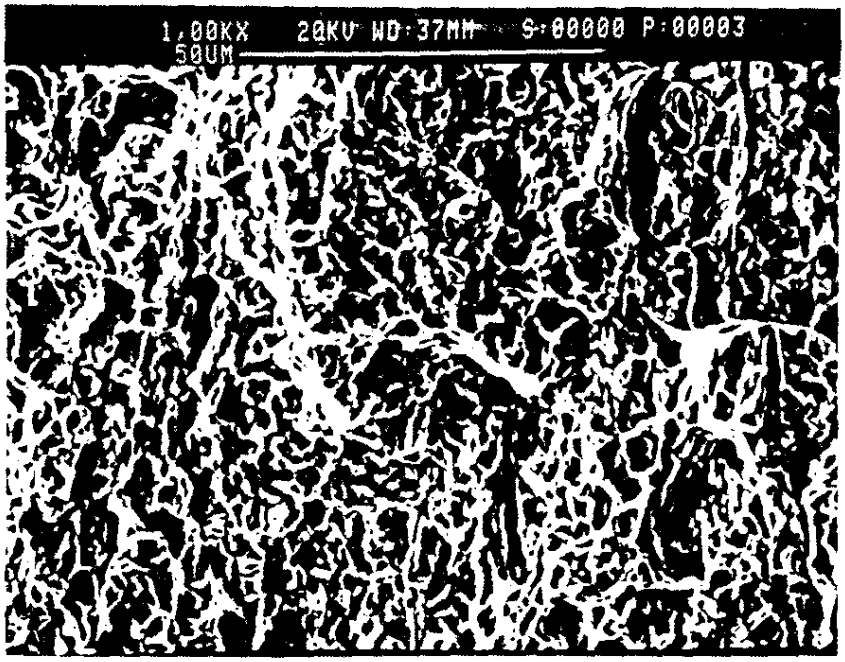

(b)

Fig. 6. Tritium and Helium Induced Fracture: (a) Transgranular in Low Toughness Microstructure; (b) Intergranular in High Toughness Microstructure.

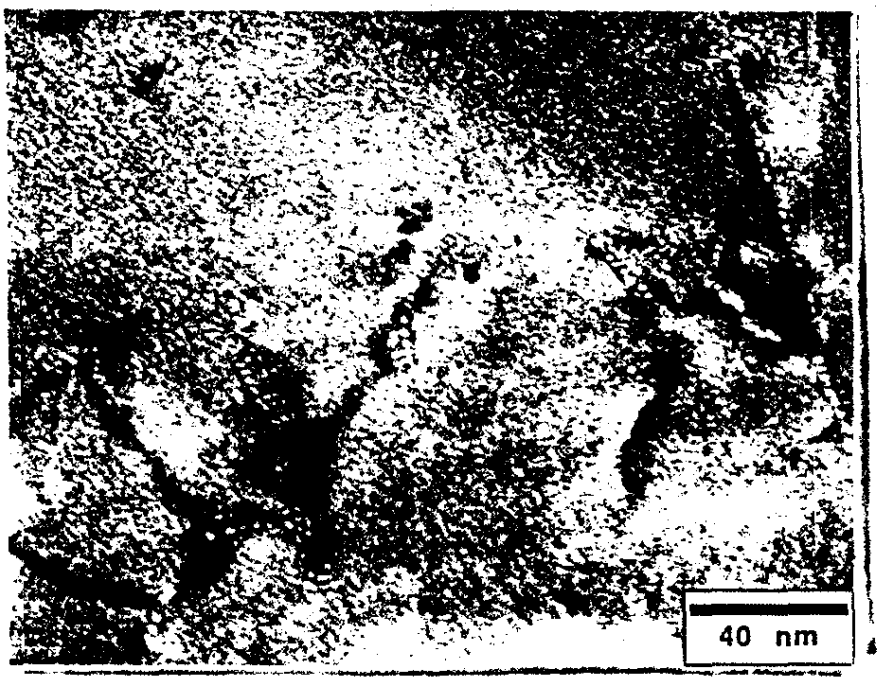

Fig. 7. Helium Bubbles in Cores of Dislocations.

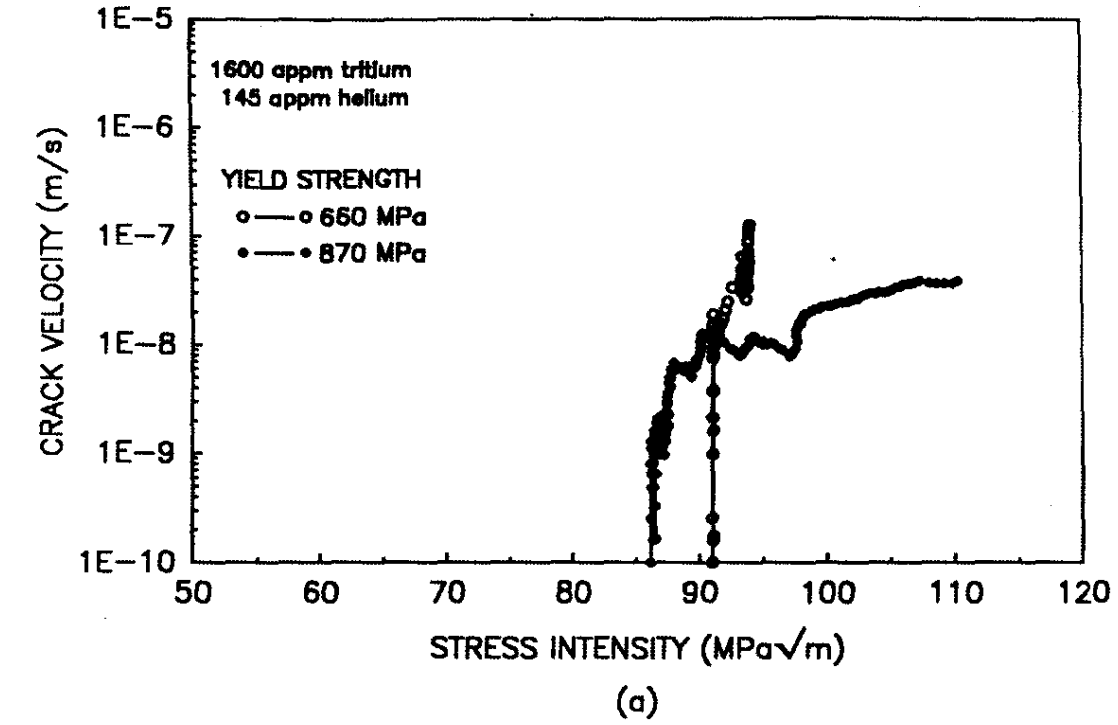

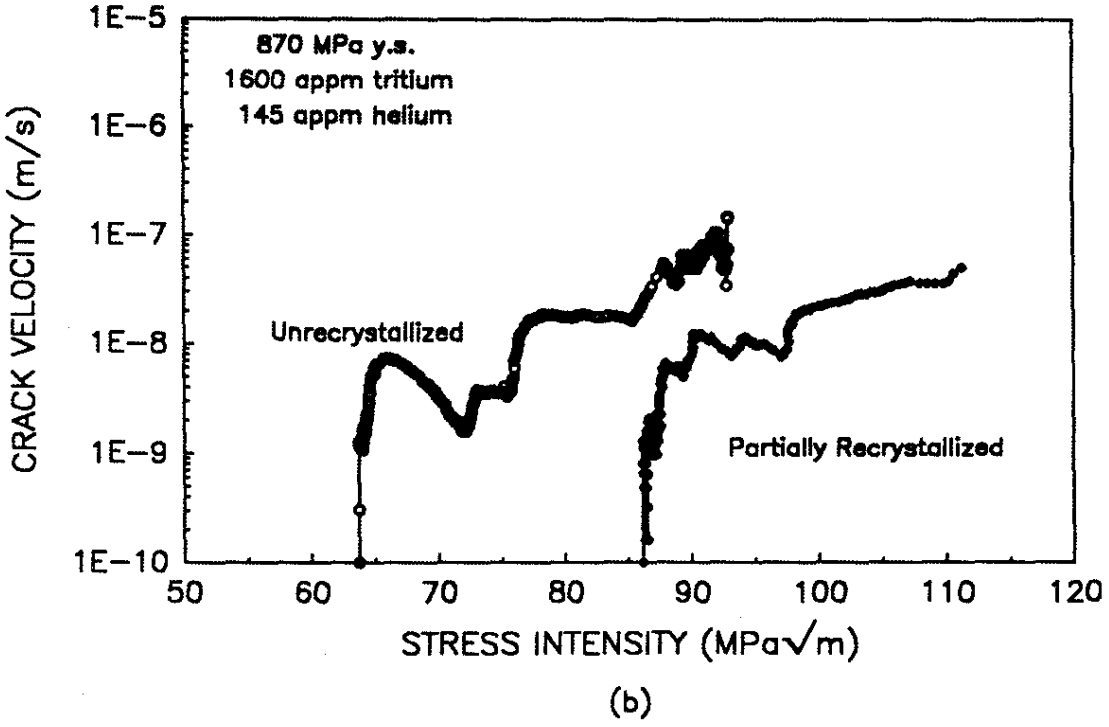

Fig. 8. Falling-Load Threshold Stresss Intensities and Crack Growth Rates in Tritium-Exposed 21-6-9: (a) Effect of Yield Strength; (b) Effect of Microstructure.